Proceeding of the IEEE
International Conference on Robotics and Biomimetics
Dali, China, December 2019

Bio-inspired Soft Robot Driven by Transparent Artificial Muscle*

Yuzhe Wang, Ujjaval Gupta and Jian Zhu
Department of Mechanical Engineering
National University of Singapore
117575, Singapore
mpezhuj@nus.edu.sg

Pengcheng Li, Donghe Du, Lei Zhang and Jianyong Ouyang
Department of Materials Science and Engineering
National University of Singapore
117574, Singapore
mseoj@nus.edu.sg

Jun Liu and Choon Chiang Foo
Institute of High-Performance Computing
Agency for Science, Technology and Research
138632, Singapore

***Abstract* - Transparency is one of the few forms of camouflage used by natural creatures in a habitat with any backgrounds. Dielectric elastomer actuators (DEAs) have important applications in many areas such as soft robots, artificial muscles and compliant devices. However, conventional DEAs cannot mimic the transparent appearance of natural creatures by using conventional materials like carbon grease as the compliant electrodes since carbon grease is a viscous black fluid. In this work, transparent artificial muscles are demonstrated by exploiting blends of poly(3,4-ethylenedioxythiophene): poly(styrenesulfonate) (PEDOT:PSS) and waterborne polyurethane (WPU) as compliant electrodes. The PEDOT:PSS/WPU blends are conductive and transparent solids, and the dielectric elastomer actuator artificial muscles can achieve a voltage-induced area strain of 200% with a transmittance of higher than 88% over the entire visible light spectrum. A transparent soft robot driven by these transparent artificial muscles is demonstrated. The fully transparent robot can vibrate asymmetrically at specific frequencies and demonstrate translational motion while keeping camouflaged in colorful backgrounds. The finite element analysis and experiments reveal the working mechanisms of the robot consistently. The concept of transparent actuators and transparent soft robots can guide the design of next-generation soft robots.**

Index Terms – artificial muscles, transparent, conducting polymer, dielectric elastomer actuator, soft robot

I. INTRODUCTION

Nature offers countless examples of camouflage, and common camouflaging strategies used by the species are background matching, disruptive coloration, and disguise [1]. Among them, transparency is one of the few forms of camouflage possible in a habitat with any backgrounds, and it conveys excellent disguise under ambient light conditions, greatly reducing the animal's visibility and the chances of being preyed. Many animals, such as species living in the pelagic region of the open ocean (such as the box jellyfish and the telescope octopus) have adapted transparency as their common trait for camouflage [2]–[5]. For example, aglama okeni (also known as Portuguese man of war) maintains a mostly transparent body with small pigmented regions to mimic small larval fish acting as lures. The approaching prey cannot identify the most disguised transparent animal [5]. Some cephalopods such as squids and octopus can also quickly switch between transparency and opaque according to the predator they are trying to escape from [6].

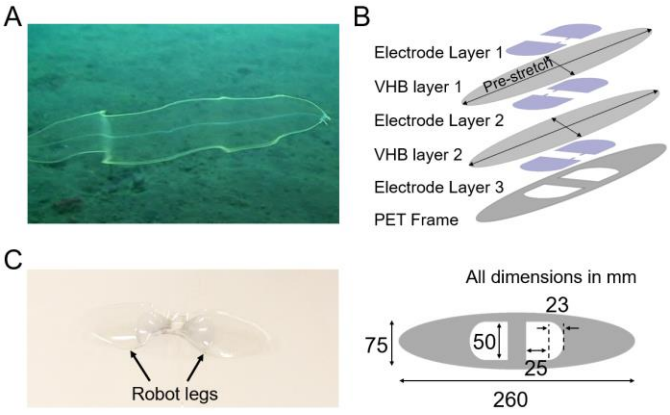

Fig. 1 (A) Transparent leptocephali in nature. (B) Design of the transparent soft robot. (C) A transparent soft robot with thin thickness and high transparency on a white background.

In the other research field, soft robots have gained great attention recently due to their potentials in many applications. Soft materials made of elastomers have been shown to effectively mimic functions of human and animal muscles because they can be triggered by simple actuation mechanisms such as pneumatic pressure, hydraulic pressure, temperature or voltage. Among them, dielectric elastomer actuators (DEAs) belong to the class of soft actuators which response to electrical stimuli. A DEA consists of a dielectric elastomer layer with two compliant electrodes on either side. When

* This work was supported in part by MOE Tier 1, Singapore under Grant R-265-000-609-114 and in part by A*STAR, Singapore under Grant R-265-000-629-305.

978-1-7281-6321-5/19//$31.00 ©2019 IEEE

subject to voltage, positive and negative charges spread across the two electrode layers respectively. The membrane consequently experiences strong Maxwell stress squeezing it in the thickness direction and simultaneously expanding in area [7]–[9]. It is of great interests that DEA based soft robots have great potential to mimic the transparent nature of the animal's camouflage behaviour. If the compliant electrodes are transparent, it can lead to the realization of transparent artificial muscles which can be effective in the development of transparent soft robots based on DEAs. To date, a couple of transparent solid conductors were investigated as the compliant electrode for DEAs, such as carbon nanotubes, graphene, elastomer/metallic nanocluster composites, and silver nanowires [10]–[17]. Nevertheless, they have problems of low transparency, low mechanical stretchability, and/or complicate fabrication process. Recently, ionically conductive hydrogels were demonstrated as the transparent electrodes for soft actuators [17], [18]. However, although the soft actuators with ionically conductive gels can exhibit high transparency and contribute to large area strain, the quasi-solid hydrogels are not in solid form and sensitive to the humidity and temperature. Therefore, it is significant to develop novel solid compliant electrode with high transparency for dielectric elastomer actuators and other stretchable systems.

Poly(3,4-ethylenedioxythiophene):poly(styrenesulfonate) (PEDOT:PSS) is an intrinsically conductive polymer which consists of two ionomers. One component in the PEDOT:PSS mixture is sodium polystyrene sulfonate where part of the sulfonyl groups are deprotonated and carry a negative charge. The other component PEDOT is a conjugated polymer and carries positive charges. Together the charged macromolecules form a macromolecular salt. Recently, PEDOT:PSS has attracted great attention since they are highly conductive and flexible. It can be coated on various substrates and nanostructures to form a composite with high electrochemical properties, thus provides a feasible solution for transparent dielectric elastomer actuators. In the recent development, PEDOT:PSS based electrodes exhibited advantages of excellent solution processability, high conductivity and high transparency in the visible range, leading to becoming a promising candidate for transparent soft actuators and soft robots [19]. In this work, a fully transparent soft robot based on transparent dielectric elastomer actuators is demonstrated by using blends of PEDOT:PSS and water-borne polyurethane (WPU) as the compliant electrodes (Fig. 1C). The actuator can achieve a voltage-induced area strain of 200% with a transmittance greater than 80% in the entire visible light spectrum. The fully transparent soft robot which has the capability of passive camouflage is fabricated by using polyethylene terephthalate (PET) and transparent DEA-based artificial muscles. The entire robot is fully transparent with very low visibility in different backgrounds. When subject to voltage with certain frequency and amplitude, the robot can move along a straight line or turning around.

II. Fabrication of Transparent Soft Robot

A PET sheet is cut into the shape illustrated in Fig. 1B by laser cutting. A VHB4910 film is prestretched radially to four times and deposited with PEDOT:PSS/WPU electrodes by spin coating on both sides, and another identical VHB film was deposited with PEDOT:PSS/WPU electrodes on only one side. The transparent robots are fabricated by separately adhering these two VHB films on the same side of a non-stretchable but highly flexible PET frame. The electrode area on the VHB film is coincident with the blanks on the PET sheet. The multi-layer structure is illustrated in Fig. 1B. The surrounded VHB is then removed with a blade from the edge of the PET sheet so that the robot can be taken out from the surrounding pre-stretched film. Before being taken out, the robot is in the mechanically constrained state with a flat shape. After removing the surrounding prestretched VHB films, the robot is self-deformed to a saddle-like shape which is its released state. The transition of the two states can be explained by the theory of dielectric elastomer minimum energy structures (DEMEs) [20], [21]. DEMEs are a subclass of dielectric elastomer actuators where the spring element is an inextensible, compliant planar frame (PET frame in this work). When the dielectric elastomer films adhere to the PET frame, the elastic energy of the dielectric elastomer film is transferred to the frame, which causes the entire system to buckle and form the shape of released state (Fig. 1C). This conformation of the film-frame system is a local minimum energy state. When a voltage is applied across the membranes of the actuators, the stresses of the membranes are increased and thus increase their strain energy. The strain energy added to the membrane results in the release of the bending energy stored in the PET frame. Thus, the whole structure tends to return to its original shape (i.e. flat shape in this case). A new minimum energy configuration is then achieved in this state. If subject to AC voltages, this process will repeat cyclically and result in vibration.

III. Transparent Soft Actuators

A. *Materials preparation and actuator fabrication*

To fabricate the transparent electrodes, PEDOT:PSS aqueous solution (Clevios PH 1000 Lot 2015P0052, 1.3wt% concentration, Heraeus) is added with 5 vol% DMSO, which is then mixed with 10 wt% WPU aqueous solution (WPU-3-505G, 39.8 wt% concentration, Taiwan PU Corporation). The loading of PEDOT:PSS in the PEDOT:PSS/WPU blends is 5wt%. Zonyl® FSO is added into the PEDOT:PSS/WPU with a concentration of 4 mg/mL. The Zonyl® FSO is used to adjust the wettability of the PEDOT:PSS/WPU water dispersion on the surface of VHB film and meanwhile acts as a plasticizer to makes the PEDOT:PSS electrode softer [22]. The prepared solution is used for the preparation of the compliant electrodes.

To illustrate the actuation ability of the transparent artificial muscles based on PEDOT:PSS/WPU electrodes, a circular DEA is fabricated to test the voltage-induced area strain. In the fabrication process, a VHB film is prestretched radially to four times of its original radius and fixed onto a

circular rigid acrylic frame of an inner diameter of 12 mm. The prepared PEDOT:PSS/WPU solution is spin-coated on both sides of the prestretched VHB film. The fabricated actuator is then dried at 60 °C for 30 min. The dried PEDOT:PSS/WPU films can adhere firmly to the VHB film, and the compliant electrodes are connected to copper stripes for electrical tests.

B. Properties of transparent electrodes and actuators

The elongation at break and mechanical modulus of the polymer blends are important in achieving large voltage-induced strain. The tensile tests show that the 5wt% PEDOT:PSS/WPU electrode suffers from the mechanical break at 416±41% linear strain (Fig. 2A), and Young's modulus is measured to be 9.7±0.3% MPa. A higher PEDOT:PSS loading in PEDOT:PSS/WPU will increase Young's modulus since PEDOT:PSS is more rigid than WPU. The Young's modulus of PEDOT/PSS/WPU electrodes used in this work is much lower than the PEDOT:PSS/WPU films with the same PEDOT:PSS loading that reported before [23], due to the addition of Zonyl® FSO fluorosurfactant as a plasticizer in the polymer blends [22].

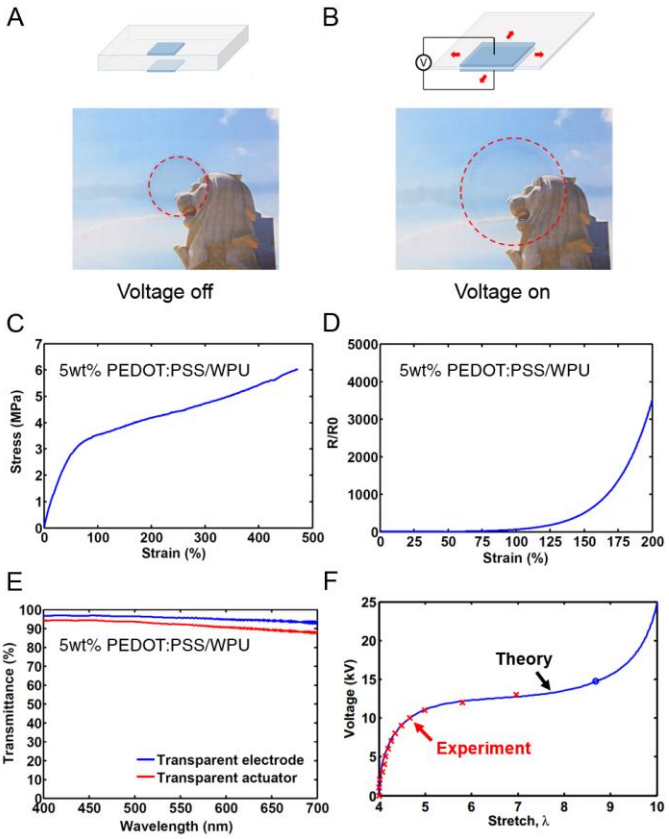

Fig. 2 A transparent dielectric elastomer actuator at (A) voltage off state and (B) voltage on state with an area strain 200%. (C) Strain-stress relation for the transparent electrode with 5wt% PEDOT:PSS loading in PEDOT:PSS/WPU blend. (D) Variations of the resistances change of PEDOT:PSS/WPU electrodes on VHB film with the tensile strain (R_0 is the resistance before stretch). (E) Transmittance of 5wt% PEDOT:PSS/WPU electrode and the transparent actuator. (F) Area strain of the DEA as a function of the applied voltage. The crosses represent the experimental data, and the simulation results represented by the blue curve are consistent with the experimental data.

The electric properties of the transparent electrode under stretch is also important for achieving high electromechanical responses. The sheet resistance of the PEDOT:PSS/WPU electrodes are measured to be 970 Ω/sq for 5wt% PEDOT:PSS/WPU. Fig. 2B shows the variations of the resistance change of the PEDOT:PSS/WPU blends on VHB films under mechanical strain. The resistance slowly increases when the strain is less than 140% for the actuators with 5wt% PEDOT:PSS/WPU (Fig. 2B), which will not significantly impede the achievement of high area strain of the actuators.

The transmittance of the dielectric elastomer actuator is measured by ultraviolet-visible spectroscopy. As the VHB film is highly transparent, the overall transmittance of the actuator is mainly dominated by the transmittance of the electrodes. The 5wt% PEDOT:PSS/WPU film exhibits an average transmittance of higher than 93% in the visible light spectrum and 95.6% at 550 nm. The transmittance of this electrode is much higher than the electrodes used for dielectric actuators in literature, such as carbon nanotube electrodes, crumpling graphene electrode, metal ion-implanted elastomer electrodes and silver nanowire-based electrodes [11], [15], [24]–[26]. The actuator consisting of two 5wt% PEDOT:PSS/WPU electrodes and a VHB film (prestretched radially to four times) exhibits a transmittance of 92% at 550 nm and a transmittance of higher than 88% in the entire visible light spectrum (Fig. 2C). The transmittance of the dielectric elastomer actuator using PEDOT:PSS/WPU electrodes is also much higher than most of the other dielectric elastomer actuators using solid electrodes, such as crumpled graphene, carbon nanotube or silver nanowire-based electrodes [10], [14], [24], [26], [27]. The excellent performance and high transmittance of the PEDOT:PSS/WPU based artificial muscle enable it to be used in fully transparent soft robots which can camouflage in the environment.

The actuation mechanism of a DEA is illustrated in the top subfigure of Fig. 2D. The bottom subfigures in Fig. 2D show that the transparent soft actuator transparent can achieve a large voltage-induced area strain of 200% when subject to a voltage of 14 kV. The dashed lines are to indicate the expansion of the active area since the electrode areas are highly transparent and hard to be identified. Fig. 2E shows the area strain of the DEA as a function of the applied voltage. The crosses represent the experimental data, and the simulation results represented by the blue curve are consistent with the experimental data. In addition, the artificial muscle can work for at least 60 thousand actuation cycles without showing any decrease in the voltage-induced area strain.

IV. Experimental Results

A. Movement of soft robot

The transparent soft robot can move along a straight line when a 5.5kV, 14Hz AC voltage is applied on the actuators. As shown in Fig. 3A, the robot is moving from the left side to the right on a white background, at a speed of 22mm/s. One can tune the amplitude and frequency of the applied voltage so that the robot can move at different speeds. We have studied

the moving mechanism of the transparent soft robot performing translational movements. The robot performs translational motion when subject to certain voltage and frequency due to asymmetric vibration of the DEMES. In addition, the robot can also perform rotational motion when the stimuli applied is a 4kV 10Hz AC voltage. In 10s, the robot rotates about 123 degrees around the geometrical center, with a rotational speed of 0.2147 rad/s.

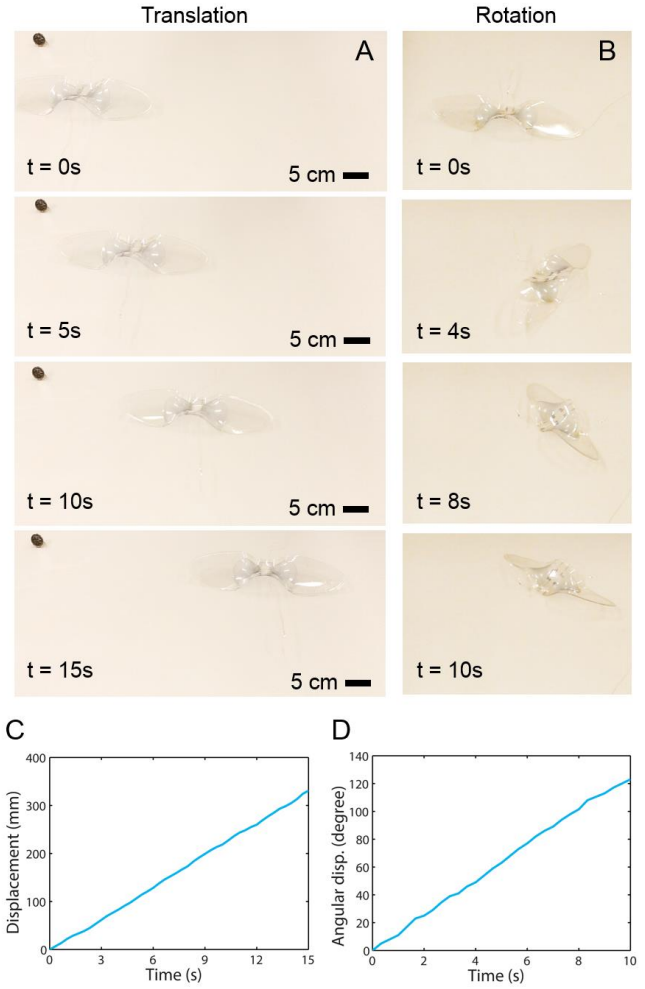

Fig. 3 (A) Transparent robot moving along a straight line. (B) Transparent robot rotating around its geometrical center. (C) Translational displacement as a function of time during translational movement. (D) Angular displacement as a function of time during rotation.

As mentioned in Section II, a DEMES can be subjected to AC voltage and excited as a dynamic system. When an AC voltage is applied to the robot, the two minimum energy states switch between each other during each half voltage cycle, causing the structure to vibrate. In physics and engineering, a dynamical system can be excited under several vibration modes. A vibration mode is a standing wave state of excitation, in which all the components of the system will be affected sinusoidally. Each mode is characterized by one or several frequencies, according to the modal variable field [28]. We apply an AC voltage with sweep frequencies from 0 Hz to 25 Hz to the robot. Experiments show that the robot performs translational motion at higher frequencies but cannot move at lower frequencies. It is reasonable to make a hypothesis that movement of this robot is characterized by its vibration modes. In experiments, amplitudes of the two robot legs (along Y-axis) are recorded. As shown in Fig. 4A, when the robot is vibrating at the symmetric mode (f < 12 Hz), amplitudes of the two legs are close to each other. When f > 12 Hz, the right leg vibrates in larger amplitudes, indicating that the robot is vibrating at its asymmetric mode.

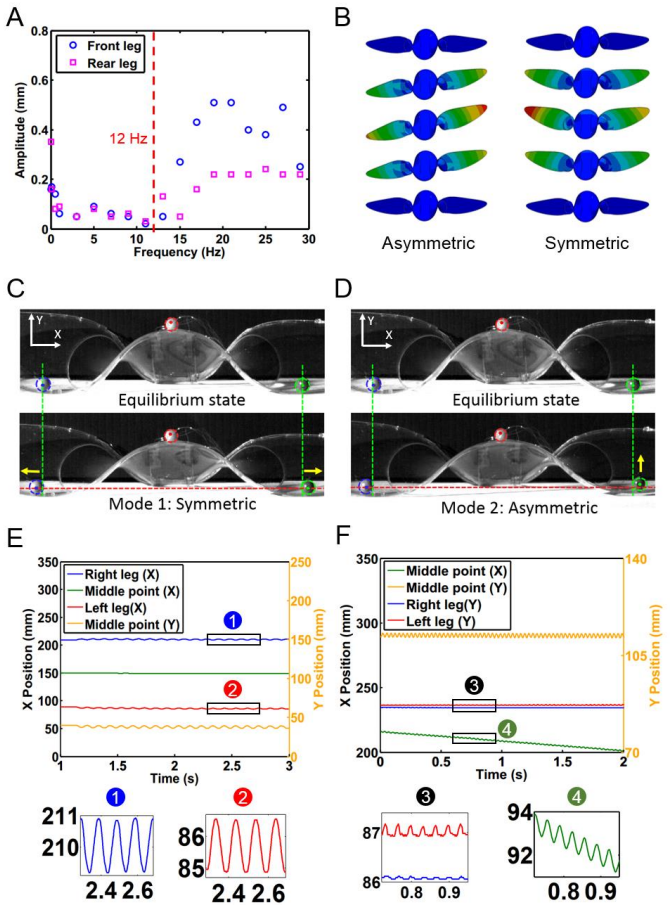

Fig. 4 (A) Amplitudes as functions of frequency under AC voltage for the two robot legs. (B) The symmetric and asymmetric vibration modes simulated by finite element method. (C) Screenshots of the high-speed camera video while the robot is vibrating at its symmetric mode. (D) Screenshots of the high-speed camera video while the robot is vibrating at its asymmetric mode. (E) Tracking results of the robot legs and mid-point when the robot is subjected to AC voltage of 4.5 kV with 5 Hz frequency. (F) Tracking results of the robot legs and mid-point when the robot is subjected to AC voltage of 4.5 kV with 14 Hz frequency.

To study the working mechanism of the robot quantitatively, high-speed camera (FASTCAM, Photron, Japan) is used to capture the video while the robot is subject to AC voltages. Videos with the applied voltage at 5Hz and 14Hz are recorded to compare the differences between the two modes. We track the motion trajectory of the two contact points (which are considered as two legs of the robot) with the

ground. Tracking records of both legs for symmetric (5Hz) and asymmetric (14Hz) vibration are shown in Fig. 4C to 4F. As shown in Fig. 4C, Y positions remain almost constant for both legs when the robot is vibrating symmetrically, indicating that the legs have no movement in the vertical direction. Meanwhile, the two legs in the horizontal direction (X position) are vibrating in opposite phases while either leg returns to its original position after each half voltage cycle (Fig. 4E). Thus, the robot is expanding and contracting cyclically but there is no relative movement between the robot and the ground. When subject to 14Hz AC voltage and vibrating asymmetrically (Fig. 4D), the right leg has larger displacement in the vertical direction than the left leg, which is indicated by a larger peak in Y position (Fig. 4F). Meanwhile, the two legs in the horizontal direction (X position) are also vibrating in opposite phases while the relative X position between either leg or the ground are increasing, implying that the entire robot body is moving towards positive X direction.

To model the dynamic behavior of the soft actuator and verify the correctness of the proposed moving mechanism, finite element method is used to simulate the two vibration modes based on the nonlinear field theory of dielectric elastomer. The finite element analysis is implemented in the commercial finite element software ABAQUS via a user-implemented material model (UMAT) [29]. The simulation results are consistent with the experimental results, as shown in Fig. 4B. Colors represent the deformation of the robot body with respect to the equilibrium state shown in blue color. When the robot is vibrating under the symmetric mode, the two legs are deforming symmetrically. However, the two legs deform asymmetrically when the robot is under the asymmetric mode. The right leg is higher than the left leg, resulting in a larger displacement in the vertical direction than the left leg.

Consequently, the moving mechanism of the robot can be explained. Translational movement only occurs when the robot is vibrating asymmetrically. During each first quarter-cycle of the applied AC voltage, the right leg moves up in the vertical direction and leaves the ground, while the left leg almost remains at its original Y position, resulting in a larger normal force on the left leg and thus larger friction force between the ground and the left leg. Meanwhile, the entire robot body expands in the horizontal direction, however, due to larger friction on the left leg, the robot tends to move towards the right (positive X direction). After that, during the second quarter-cycle, voltage is decreasing. The right leg moves down and contacts the ground again, providing larger normal force and friction force compare to the first quarter-cycle. Meanwhile, since the robot body is contracting and the right leg will contract less than expands in the first quarter-cycle, the robot will tend to move towards the right. This mechanism repeats in every half-cycle of the AC voltage applied, resulting in continuous forward movements.

B. Camouflage capability

Camouflaging in the working environment is an interesting feature which can be used for disguising the structure against the background. Some of the previous works focus on achieving camouflaging by changing colors and/or display pattens. It is an effective way to disguise but difficult to be achieved in environments where a lot of color variations are presented. The transparent and extremely thin soft robot can achieve excellent passive camouflage at either actuated state or reference state due to highly transparent artificial muscles. Fig. 5A shows the transparent robot on a colorful background of Singapore's skyline. The robot is almost invisible and camouflages very well in the background at either voltage off (buckled) or voltage on (flat) state. At the voltage on state (5.5 kV DC), the robot can turn completely flat, thus minimizing the reflections from the ambient light and achieve even better camouflage.

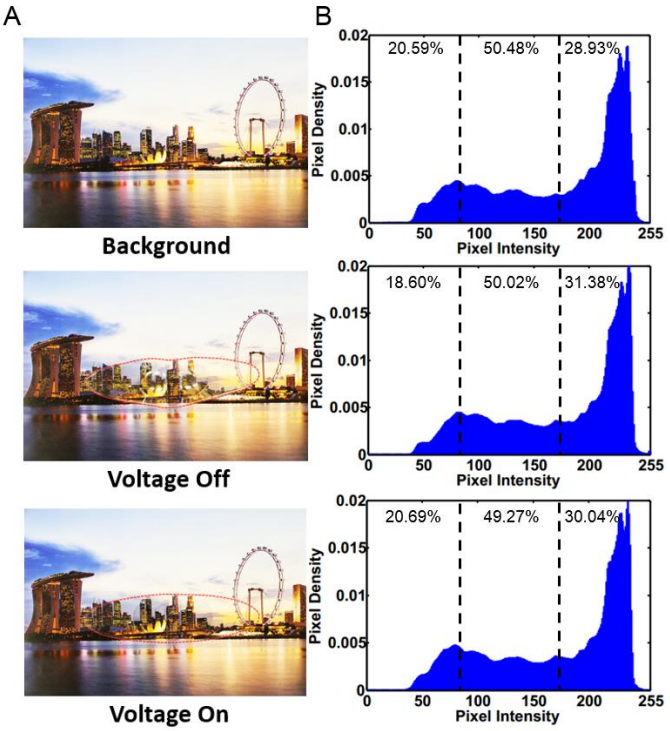

Fig. 5 (A) Images of the transparent robot at voltage off and state on colorful background and (B) histograms showing the distributions of grayscale intensities of the images.

To investigate the effectiveness of passive camouflaging, image analysis is performed using MATLAB, which can further illustrate the visibility of the robot. As shown in Fig. 5B, three histograms show the distributions of grayscale intensities of the colorful background, the robot at voltage off state and voltage on state, respectively. Each histogram is divided into three equal domains, the darker domain (<85 pixel intensity), the lighter domain (>170 pixel intensity) and the middle domain (between pixel intensity 85 and 170) with mostly grey pixels. The percentage of dark, grey and light pixels of the three images are shown in Fig. 5B. It can be observed that the pixel intensity distribution of the transparent robot at both the voltage on and the voltage off state are quite close to the background, demonstrating the effectiveness of optical camouflage. The analysis implies that the transparent

robot is able to camouflage well in the colorful environment at either voltage on or voltage off state. Furthermore, the histogram of the images at the voltage on state is even more close to that of the background, thus the robot at the voltage on state can camouflage even better in the environment.

V. Conclusion

In this work, highly transparent DEA-based artificial muscles are developed using stretchable, transparent, solid-state electrodes based on PEDOT:PSS and waterborne polyurethane. The transparent soft actuator can achieve a 200% area strain with a transmittance of higher than 88% in the visible light spectrum. The developed artificial muscles enable soft robots to be fully transparent and almost invisible on colorful backgrounds. The robot can translate or rotate by controlling the voltage while keeping camouflaged. The transparent soft robot presented in this work is one of the first transparent soft robots working on land and camouflaging in all surroundings, which is much more challenging than that in water due to larger difference in refractive index between air and robot body. This work confirms the feasibility of the PEDOT:PSS/WPU based transparent actuator to serve multiple functions in soft robots: actuation, movement, and camouflage. These machines can be used by biologists to study animal behavior such as the predator/prey relationships. The robot can also effectively hide even closer to the background by transferring to a 2D structure. By further integrating power sources, circuits and control units on the robot, an untethered system can be achieved, while the untethered system will demand more technically advanced transparent electronics, and the challenges to achieve untethered systems may be addressed by using a robot with a larger body and higher payload which can carry the electronics. Another focus of future developments can be the durability and robustness of the robot. Improvements of transparent electrodes and application of protective layers can increase the lifetime of the robot and enable the robot to operate in harsh environments. The concept of transparent artificial muscles and transparent soft robots can be used to guide the design of next-generation soft robots.

References

[1] S. A. Morin, R. F. Shepherd, S. W. Kwok, A. A. Stokes, A. Nemiroski, and G. M. Whitesides, "Camouflage and Display for Soft Machines," *Science 80*, vol. 337, no. 6096, p. 828 LP-832, Aug. 2012.

[2] M. J. Mcfall-Ngai, "Crypsis in the Pelagic Environment," *Am. Zool.*, vol. 30, no. 1, pp. 175–188, Feb. 1990.

[3] S. Johnsen, "Hidden in plain sight: the ecology and physiology of organismal transparency.," *Biol. Bull.*, vol. 201, no. 3, pp. 301–318, Dec. 2001.

[4] S. Johnsen, "Hide and Seek in the Open Sea: Pelagic Camouflage and Visual Countermeasures," *Ann. Rev. Mar. Sci.*, vol. 6, no. 1, pp. 369–392, Jan. 2014.

[5] S. Johnson, "Transparent animals.," *Sci. Am.*, vol. 282, no. February, pp. 62–71, 2000.

[6] S. Zylinski and S. Johnsen, "Mesopelagic cephalopods switch between transparency and pigmentation to optimize camouflage in the deep," *Curr. Biol.*, vol. 21, no. 22, pp. 1937–1941, Nov. 2011.

[7] R. Pelrine, R. Kornbluh, and G. Kofod, "High-strain actuator materials based on dielectric elastomers," *Adv. Mater.*, vol. 12, no. 16, pp. 1223–1225, 2000.

[8] B. Chen *et al.*, "Highly stretchable and transparent ionogels as nonvolatile conductors for dielectric elastomer transducers," *ACS Appl. Mater. Interfaces*, vol. 6, no. 10, pp. 7840–7845, 2014.

[9] S. J. A. Koh *et al.*, "Mechanisms of large actuation strain in dielectric elastomers," *J. Polym. Sci. Part B Polym. Phys.*, vol. 49, no. 7, pp. 504–515, Apr. 2011.

[10] W. Yuan *et al.*, "Fault-tolerant dielectric elastomer actuators using single-walled carbon nanotube electrodes," *Adv. Mater.*, vol. 20, no. 3, pp. 621–625, 2008.

[11] V. Scardaci, R. Coull, and J. N. Coleman, "Very thin transparent, conductive carbon nanotube films on flexible substrates," *Appl. Phys. Lett.*, vol. 97, no. 2, p. 023114, 2010.

[12] S. Shian, R. M. Diebold, A. McNamara, and D. R. Clarke, "Highly compliant transparent electrodes," *Appl. Phys. Lett.*, vol. 101, no. 6, p. 061101, 2012.

[13] T. Hwang *et al.*, "Transparent actuator made with few layer graphene electrode and dielectric elastomer, for variable focus lens," *Appl. Phys. Lett.*, vol. 103, no. 2, p. 023106, 2013.

[14] J. B. Pyo *et al.*, "Floating compression of Ag nanowire networks for effective strain release of stretchable transparent electrodes," *Nanoscale*, pp. 16434–16441, 2015.

[15] S. Rosset, M. Niklaus, P. Dubois, and H. R. Shea, "Metal ion implantation for the fabrication of stretchable electrodes on elastomers," *Adv. Funct. Mater.*, vol. 19, no. 3, pp. 470–478, 2009.

[16] S. Rosset and H. R. Shea, "Flexible and stretchable electrodes for dielectric elastomer actuators," *Appl. Phys. A Mater. Sci. Process.*, vol. 110, no. 2, pp. 281–307, 2013.

[17] C. Keplinger, J.-Y. Sun, C. C. Foo, P. Rothemund, G. M. Whitesides, and Z. Suo, "Stretchable, Transparent, Ionic Conductors," *Science 80*, vol. 341, no. 6149, pp. 984–987, 2013.

[18] B. Chen *et al.*, "Stretchable and transparent hydrogels as soft conductors for dielectric elastomer actuators," *J. Polym. Sci. Part B Polym. Phys.*, vol. 52, no. 16, pp. 1055–1060, 2014.

[19] P. Li *et al.*, "Transparent Soft Robots for Effective Camouflage," *Adv. Funct. Mater.*, vol. 1901908, p. 1901908, 2019.

[20] M. T. Petralia and R. J. Wood, "Fabrication and analysis of dielectric-elastomer minimum-energy structures for highly-deformable soft robotic systems," in *2010 IEEE/RSJ International Conference on Intelligent Robots and Systems*, 2010, pp. 2357–2363.

[21] G. Kofod, W. Wirges, M. Paajanen, and S. Bauer, "Energy minimization for self-organized structure formation and actuation," *Appl. Phys. Lett.*, vol. 90, no. 8, p. 081916, 2007.

[22] S. Savagatrup *et al.*, "Plasticization of PEDOT:PSS by Common Additives for Mechanically Robust Organic Solar Cells and Wearable Sensors," *Adv. Funct. Mater.*, vol. 25, no. 3, pp. 427–436, Jan. 2015.

[23] P. Li, D. Du, L. Guo, Y. Guo, and J. Ouyang, "Stretchable and conductive polymer films for high-performance electromagnetic interference shielding," *J. Mater. Chem. C*, vol. 4, no. 27, pp. 6525–6532, 2016.

[24] L. Hu, W. Yuan, P. Brochu, G. Gruner, and Q. Pei, "Highly stretchable, conductive, and transparent nanotube thin films," *Appl. Phys. Lett.*, vol. 94, no. 16, p. 161108, 2009.

[25] S. Yun, X. Niu, Z. Yu, W. Hu, P. Brochu, and Q. Pei, "Compliant silver nanowire-polymer composite electrodes for bistable large strain actuation," *Adv. Mater.*, vol. 24, no. 10, pp. 1321–1327, 2012.

[26] J. Zang *et al.*, "Multifunctionality and control of the crumpling and unfolding of large-area graphene.," *Nat. Mater.*, vol. 12, no. 4, pp. 321–325, 2013.

[27] J. Wang, C. Yan, K. J. Chee, and P. S. Lee, "Highly stretchable and self-deformable alternating current electroluminescent devices," *Adv. Mater.*, vol. 27, no. 18, pp. 2876–2882, 2015.

[28] R. D. Blevins, "Formulas for Natural Frequency and Mode Shape," *J. Acoust. Soc. Am.*, vol. 67, no. 5, pp. 1849–1849, May 1980.

[29] C. C. Foo and Z.-Q. Zhang, "A Finite Element Method for Inhomogeneous Deformation of Viscoelastic Dielectric Elastomers," *Int. J. Appl. Mech.*, vol. 7, no. 05, p. 1550069, 2015.